Analysis of wildfires using GIS technologies (case study of Volyn region, Ukraine)

Olga Artemenko[1,†], Serhii Puhach[2,†], Oleh Kaidyk[3,*,†], Taras Terletskyi[3,†] and Nina Zdolbitska[3,†]

[1] *Private Higher Educational Institution "Bukovinian university", Ch. Darvina Street 2a, 58000 Chernivtsi, Ukraine*
[2] *Lesia Ukrainka Volyn National University, Volya Avenue 13, 43025 Lutsk, Ukraine*
[3] *Lutsk National Technical University, Lvivska Street 75, 43018 Lutsk, Ukraine*

Abstract

The paper proposed a GIS-based study, which allow analysis of the impact of wildfires using multispectral satellite images. A wildfire that occurred between 30 April and 3 May 2025 north of the village Birky, Kamin-Kashirsky district Volyn region (northwestern Ukraine), formed the basis of the study. Using channels in the near-infrared (NIR) and short-wave infrared (SWIR) ranges was found to be the most promising approach for promptly detecting wildfires and determining their long-term consequences. To interpret the study results, consequences and intensity of the wildfire were assessed using the US Geological Survey scale and a normalized burning coefficient. Creating forest fire intensity maps is key to developing vegetation restoration plans after fires and assessing the potential future impact on burnt areas.

Keywords

Geographic information system (GIS), wildfires, remote sensing, normalized burn ratio, QGIS, Volyn region.

1. Introduction and problem statement

Wildfires are among the most dangerous natural disasters today. They are caused by both natural and anthropogenic factors. In any case, they lead to significant economic, environmental, and socio-cultural losses. In the context of modern climate change and rising air temperatures, the intensity of forest and steppe fires is increasing. Traditional monitoring methods often prove to be ineffective due to the vastness of the studied areas, the time lag between the start of a fire and its detection, and limited access to certain territories. In this context, remote sensing methods, particularly satellite image analysis, offer new opportunities for timely detection, impact assessment, and fire forecasting. Satellite data makes it possible to cover large areas, quickly (often in real time) identify thermal anomalies, analyse potential burned areas, and track wildfire spread dynamics. The widespread use of geographic information systems (GIS) and technologies opens up new possibilities for processing, analyzing, and visualizing a wide range of wildfire data. This integration of diverse information provides valuable support for decision-making. All of the above highlights the importance of studying wildfires using GIS and remote sensing, especially given the limited number of such studies in Ukraine.

The objective of this work is to analyze the potential of remote sensing data and various web services for wildfire analysis using GIS technologies, with a focus on the Volyn region of Ukraine.

The main tasks of the study are: to find the needed satellite images using web services such as Copernicus Browser and Earth Explorer; to analyze the image bands from Sentinel-2 (European Space Agency) and Landsat 8 (NASA) satellites for fire detection and analysis; to calculate the

AIT&AIS'2025: International Scientific Workshop on Applied Information Technologies and Artificial Intelligence Systems, December 18–19 2025, Chernivtsi, Ukraine
[1,*] Corresponding author.
[†] These authors contributed equally.
olga.hapon@gmail.com (O. Artemenko); puhachserhiy@gmail.com (S. Puhach); o.kaidyk@lntu.edu.ua (O. Kaidyk); t.terletskyi@lntu.edu.ua (T. Terletskyi); n.zdolbitska@lutsk-ntu.com.ua (N. Zdolbitska)
0000-0002-4057-1217 (O. Artemenko); 0000-0002-3738-7961 (S. Puhach); 0000-0002-3620-270X (O. Kaidyk); 0000-0002-4114-0734 (T. Terletskyi); 0000-0002-1345-3581 (N. Zdolbitska)

Normalized Burn Ratio (NBR) and delta Normalized Burn Ratio (dNBR) for calculating the fire impact; to identify the advantages and limitations of Sentinel-2 and Landsat 8 imagery in analyzing wildfire consequences, using the example of the wildfire near the village of Birky, Kamin-Kashyrskyi district, Volyn region, Ukraine.

2. Related work

In modern scientific literature, there are numerous publications dedicated to this issue. For instance, F. Sivrikaya et al., based on their analysis of Mediterranean forest areas in Turkey (in the Yeşilova Forestry Enterprise, Kahramanmaraş), described the potential of GIS for analyzing and assessing forest fire risk while accounting for factors such as tree species composition, forest cover percentage, stand age, slope steepness, aspect, and distance from settlements and roads. They also analyzed the visibility of fire watchtowers used for forest monitoring in the study area [1].

R. Jaiswal et al., using ArcGIS software and forest data from the Gorna Subwatershed (Madhya Pradesh, India), developed a GIS-based model to assess wildfire risk across the study region. A color composite image from the Indian Remote Sensing Satellite (IRS) 1D LISS III was used for vegetation mapping. Based on the dataset, four wildfire-risk zones were identified. The recommended GIS model appeared to be very useful with the actual fire-affected areas [2].

E. Chuvieco and J. Salas recommended mapping fires in Central Spain using GIS and comparing wildfire maps with topographic, meteorological, vegetation, and human activity maps. Three maps were created-probability of ignition, fuel hazard, and human risk-which were integrated into a comprehensive fire danger map based on Spanish Forest Service criteria. This approach improved understanding of spatial fire distribution, which has critical results for developing regional fire protection plans [3].

A. Supriadi and T. Oswari proposed a GIS-based web application for the fire department of Depok City (Indonesia). The system aimed to speed up fire report processing, present spatial and non-spatial data, update wildfire records, and assist in locating new fire stations, hydrants, wildfire-prone zones, and ignition hotspots [4].

H. Adab et al. studied fires in northeastern Iran using extreme temperature data from the MODIS satellite. As a result, they calculated several indexes-Structural Wildfire Index, Wildfire Risk Index, and Hybrid Wildfire Index-for monitoring and minimizing wildfire occurrence and related damage. Key wildfire-contributing factors included proximity to settlements and roads, slope steepness and aspect, elevation, and vegetation moisture. All of the listed previously factors were incorporated into a GIS model [5].

In Ukraine, some attention has also been given to studying wildfire using GIS and remote sensing. V. Zatserkovnyi and others examined the use of satellite imagery for forest wildfire monitoring through remote sensing and highlighted the advantages of this data for detecting wildfire and assessing their impact on ecosystems. A range of morphometric analyses and index calculations were conducted, with image classification performed using the Maximum Likelihood method [6].

Researchers from Lviv Polytechnic National University studied wildfires in the Chornobyl Exclusion Zone in 2020 using Sentinel-2 satellite data [7]. They applied the Normalized Burn Ratio (NBR) and supervised classification methods to identify fire-damaged areas and quickly assess wildfire impacts. Their findings showed that the NBR-based calculation had an error margin of 6.7% relative to reference area values, which is acceptable for this type of task, while supervised classification yielded lower accuracy (11.5%) but allowed identification of multiple land-cover classes.

O. Borysenko and V. Meshkova addressed fire and pest outbreak prediction in pine forests using GIS technologies in their monograph [8]. They proposed developing a forest protection and pest monitoring subsystem within the national information system “Forests of Ukraine”.

A study by O. Bandurko and O. Svynchuk focused on identifying wildfires using low-resolution satellite images and a “fire pixel” detection algorithm for TERRA MODIS and NOAA AVHRR data

[9]. Based on the Chornobyl Exclusion Zone and nearby areas, the researchers concluded that for accurate wildfire identification, cloud-covered and water-covered fragments should be excluded from image interpretation. The practical method combined mid-infrared (3–4 μm) and thermal (10–11 μm) data, enabling rapid real-time wildfire detection at subpixel resolution.

As seen from Ukrainian studies, most research focuses on wildfires in the Chornobyl Exclusion Zone, while other regions remain largely unexplored. Therefore, the study of wildfires in Ukraine using GIS tools is still underdeveloped and requires further investigation.

3. Methods and materials

The source base of this study consists of freely available satellite images from the European Space Agency (ESA) and NASA. We analyzed multispectral satellite images to detect and study wildfires. This can be done through online platforms designed for working with satellite data, such as Copernicus Browser (a free ESA resource) [10] and Earth Explorer (a free NASA resource) [11]. Another option is to download the imagery and analyze it in a GIS environment (e.g., QGIS). Modern GIS software supports direct image downloads, such as through the Semi-Automatic Classification Plugin (SCP) for QGIS. However, from our point of view, Copernicus Browser and Earth Explorer are more convenient because they allow users to preview satellite images before downloading and perform basic analyses directly within the platforms.

Copernicus Browser is a free online application that provides easy access to satellite imagery from Copernicus missions and combined datasets. Because of how easy it is to use and its intuitive interface allows any user to explore the planet easily using high-resolution satellite data. The platform provides ready-to-use imagery, preset visualizations, and thematic data collections. Copernicus Browser allows visualization of Sentinel-2 imagery in several modes, such as: True Color (bands B4, B3, B2); False Color (bands B8, B4, B3); False Color (Urban) (bands B12, B11, B4); Highlight Optimized Natural Color.

Various spectral indices, including: Normalized Difference Vegetation Index (NDVI) = (B8 − B4) / (B8 + B4); Moisture Index = (B8A − B11) / (B8A + B11); Normalized Difference Water Index (NDWI) = (B3 − B8) / (B3 + B8); Normalized Difference Snow Index (NDSI) = (B3 − B11) / (B3 + B11); Scene Classification Map (Sentinel-2 data processed with the ESA algorithm).

Each band represents a specific range of the electromagnetic spectrum, and the satellite sensor captures Earth's surface in these spectral ranges. Users can also define custom band combinations or scripts, create time-lapse animations (e.g., for vegetation dynamics, land use, or urban growth), perform basic measurements and calculations, and export results in multiple formats [12].

The USGS Earth Explorer data portal provides access to geospatial datasets from the U.S. Geological Survey. Users can search by location or coordinates to obtain Landsat satellite imagery, radar data, UAS data, digital elevation models, aerial photos, and other geospatial datasets. Earth Explorer supports visualization of Landsat 8–9 imagery in multiple modes, including: Reflective Color (bands 6, 5, 4); Thermal Browse (band 10); Quality Browse; Natural Color (bands 4, 3, 2); Color Infrared (CIR) (bands 5, 4, 3); False Color (Urban) (bands 7, 6, 5); False Color (Vegetation Analysis) (bands 6, 5, 4); Near Infrared (NIR) (band 5); Normalized Burn Ratio (NBR); Normalized Difference Moisture Index (NDMI); Normalized Difference SnowIndex (NDSI); Normalized Difference Vegetation Index (NDVI); Soil Adjusted Vegetation Index (SAVI); Thermal Band Average (bands 10, 11); Thermal (band 11).

Comparing Copernicus Browser and Earth Explorer, their basic visualization tools are similar. However, Copernicus Browser provides greater flexibility for preliminary data analysis directly within the platform.

To assess wildfire impact and burn severity, the Normalized Burn Ratio (NBR) is used, calculated as:

$$NBR = \frac{NIR - SWIR}{NIR + SWIR}, \quad (1)$$

where: *NBR* – Normalized Burn Ratio; *NIR* – Near-infrared reflectance (Sentinel-2: Band 8; Landsat 8–9: Band 5); *SWIR* – Shortwave infrared reflectance (Sentinel-2: Band 12; Landsat 8–9: Band 7) [13].

To evaluate burn severity, the difference between pre-wildfire and post-wildfire NBR, called delta NBR (dNBR), is calculated:

$$dNBR = prefire\ NBR - postfire\ NBR, \tag{2}$$

where: *dNBR* – delta Normalized Burn Ratio; *prefire NBR* – NBR before the fire; *postfire NBR* – NBR after the fire.

Higher dNBR values indicate more severe burn damage, while negative values may suggest vegetation regrowth after the wildfire [13].

Burn severity classification was created using the scale proposed by the United States Geological Survey (USGS) (Table 1).

Table 1
Ordinal severity levels and example range of dNBR (scaled by 1000) [14]

Severity level	dNBR range
Enhanced regrowth, high	-500 to -251
Enhanced regrowth, low	-250 to -101
Unburned	-100 to +99
Low severity	+100 to +269
Moderate-low severity	+270 to +439
Moderate-high severity	+440 to +659
High severity	+660 to +1300

4. Experiment

Our area of interest for this study is a wildfire in northwestern Ukraine [15]. The exact location of the event is north of the village of Birky, Kamin-Kashyrskyi District, Volyn Region. The fire lasted four days, from April 30 to May 3, 2025.

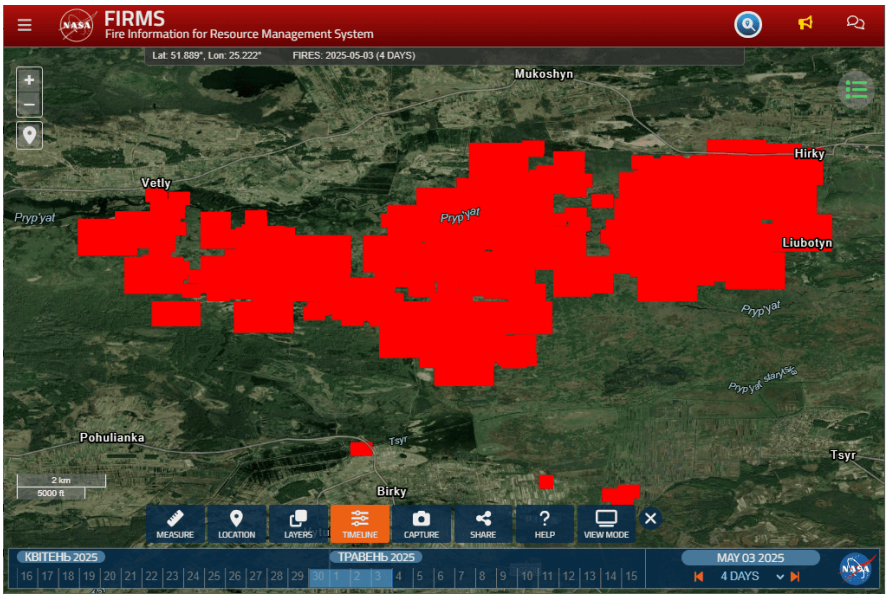

Figure 1: Fires near Birky village (Volyn Region, Ukraine), April 30-May 3, 2025 (FIRMS data) [17].

The previous location of the wildfire (approximate boundary determination) and its duration were established using the FIRMS (Fire Information for Resource Management System) web service (Fig. 1) [16].

To detect and analyze wildfires in the Copernicus Browser service, certain bands or combinations of bands are used. For example, Sentinel-2 satellite imagery and the band combination B12, B8, B2 [10]. These bands operate mainly in the shortwave infrared range. In these channels, our area of interest is displayed as shown in Fig. 2. Shortwave infrared bands (e.g., B12, B8, B2) allow clear identification of active burning areas and burned zones. Red and orange indicate active wildfires, while dark gray and black show burned areas. However, note that in the shortwave infrared range, water bodies (such as Lake Rohizne north of Vetly village) also appear black. Heavy smoke and cloud cover somewhat hides image interpretation (Fig. 2).

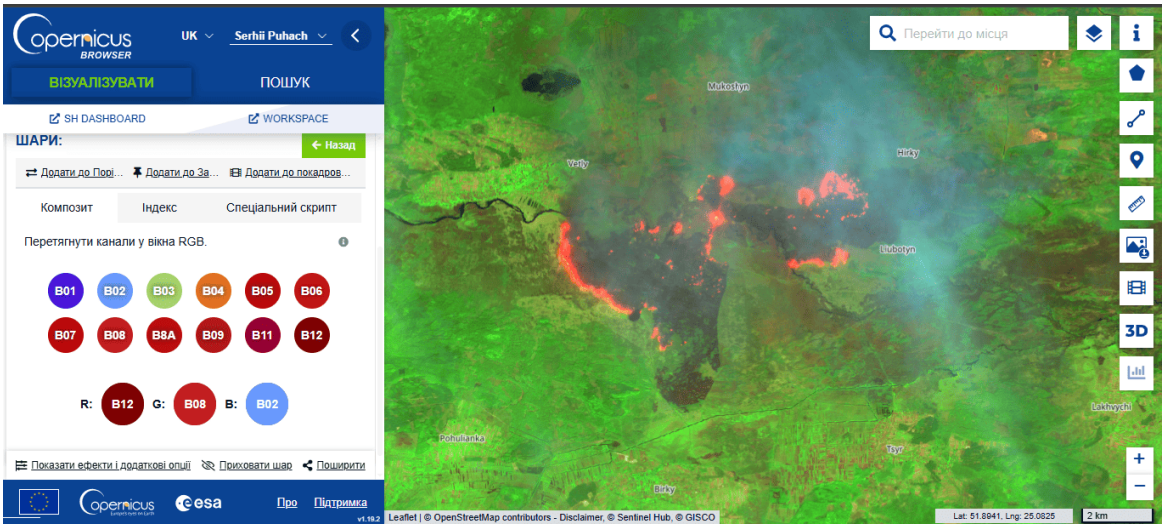

Figure 2: Visualization of the fire near Birky (Volyn Region, Ukraine) in Copernicus Browser, May 2, 2025 (Sentinel-2 L2A, bands B12, B8, B2) [10].

In Earth Explorer, fires are best seen using Thermal Browse (band 10), Thermal Band Average (bands 10, 11), and Thermal (band 11).

The next step is to download the satellite images. For dNBR calculations, Sentinel-2 L2A images (via Copernicus Browser) and Landsat 8-9 OLI/TIRS C2 L1 images (via Earth Explorer) were downloaded. Images were selected for both pre- and post-wildfire periods. Due to several factors-capture frequency, time of day, weather (especially cloudiness), and partial image commercialization-this task was not straightforward. The pre-wildfire images were of good quality and available for April 27, 2025 (Sentinel-2), and April 21, 2025 (Landsat 9). However, because of cloudy conditions, the first high-quality post-wildfire image was available only on June 4, 2025 (Sentinel-2) and June 16, 2025 (Landsat 8–9). This delay means that vegetation in the area (mostly wet floodplain meadows of the Pripyat River) could have already recovered. Therefore, for further analysis, we used partially cloudy images from May 7, 2025, available for both Sentinel-2 and Landsat 9 (Figs. 3, 4).

The Sentinel-2 image is of higher quality than the Landsat 9 one. This is due to Sentinel-2's better spatial resolution (20 m per pixel vs. 30 m per pixel) and newer technology (launched 2015–2017, compared to 2013 for Landsat 9). Around 10–15% of the area was covered by clouds, reducing the precision of further analysis.

Next, we determined the exact wildfire boundaries. The images were processed in QGIS 3.16.16-Hannover. A vector layer was created, and based on different image types/band combinations (True color, False color, SWIR for Sentinel-2; Reflective Color, False Color, NBR for Landsat 8–9), the wildfire perimeter was delineated. Due to limited image availability and cloud cover, images from several dates were used.

To refine the boundary, the “Fire Boundary Script” [18] was also applied. This script enhances the contrast and visibility of burned forest areas using Sentinel-2 bands B11 and B12. It highlights active wildfires in white, burned zones in gray, and darkens the rest. In our case, this yielded clear and detailed results (Fig. 5).

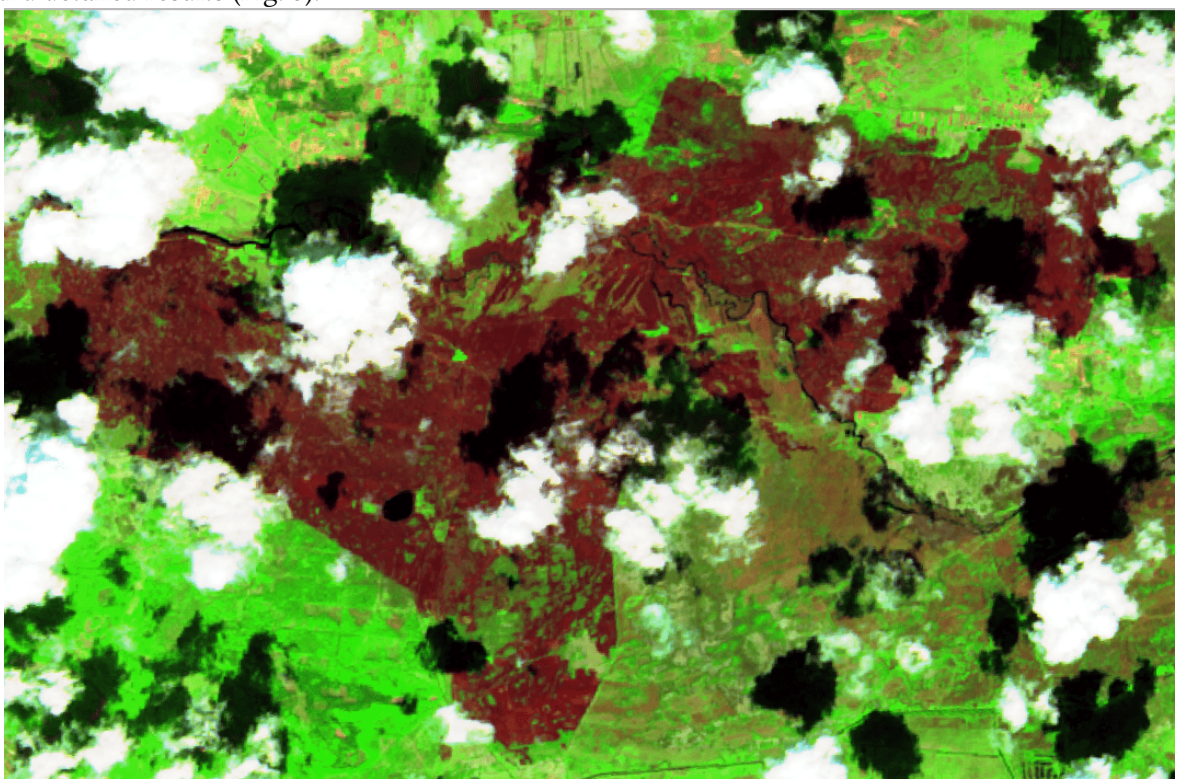

Figure 3: Satellite image of the wildfire near Birky, May 7, 2025 (Sentinel-2 L2A, bands B12, B8A, B4 (SWIR)).

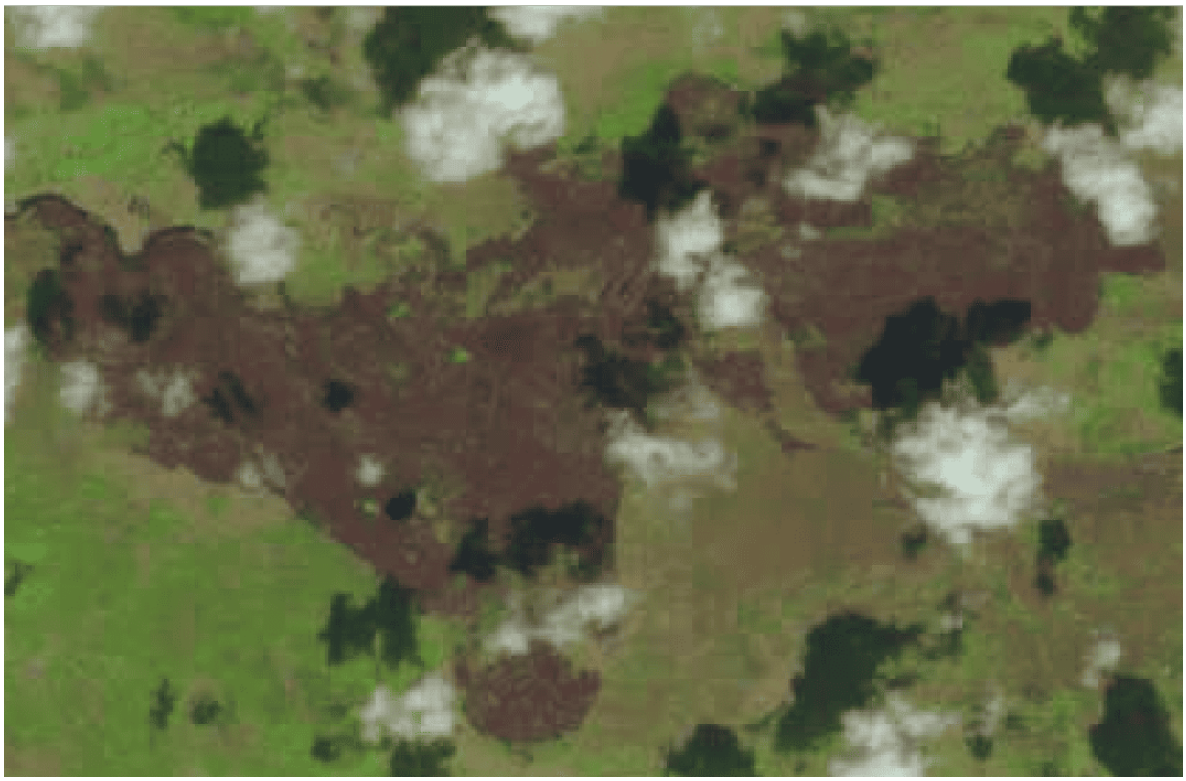

Figure 4: Satellite image of the wildfire near Birky, May 7, 2025 (Landsat 9 OLI/TIRS C2 L1, bands 6, 5, 4 (Reflective Color)).

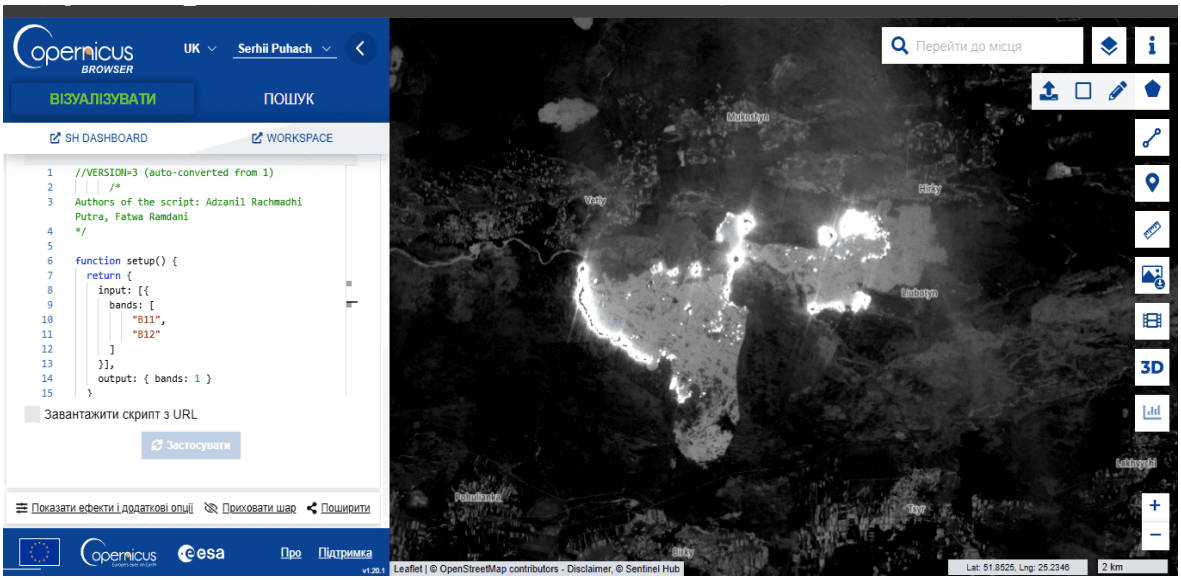

Figure 5: Visualization of the wildfire near Birky, May 2, 2025 (Copernicus Browser, Sentinel-2 L2A, Fire Boundary Script) [10].

The dNBR (differenced Normalized Burn Ratio) was calculated in QGIS 3.16.16-Hannover using the Raster Calculator plugin and formulas (1) and (2) to produce cartographic models for: 27.04.2025 – 07.05.2025 (Sentinel-2); 27.04.2025 – 04.06.2025 (Sentinel-2); 21.04.2025 – 07.05.2025 (Landsat 8–9); 21.04.2025 – 16.06.2025 (Landsat 8–9).

Example formula for Landsat 9 on May 7, 2025, in Raster Calculator:

```
(("LC09_L1TP_185024_20250421_20250421_02_T1_B5@1"-
-"LC09_L1TP_185024_20250421_20250421_02_T1_B7@1"/
/("LC09_L1TP_185024_20250421_20250421_02_T1_B5@1+
+"LC09_L1TP_185024_20250421_20250421_02_T1_B7@1"))-
-((LC09_L1TP_185024_20250507_20250507_02_T1_B5@1-
-"LC09_L1TP_185024_20250507_20250507_02_T1_B7@1"/
/("LC09_L1TP_185024_20250507_20250507_02_T1_B5@1+
+"LC09_L1TP_185024_20250507_20250507_02_T1_B7@1")).
```

Burned area sizes by damage class (Table 1) were computed in QGIS 3.16.16-Hannover using the “Raster layer unique values report” plugin.

Finally, visualization of results was done using the USGS (United States Geological Survey) classification scale for interpreting burn severity (Table 1). The threshold for wildfire-affected vegetation was set at dNBR = 100. Based on this threshold, the wildfire perimeter was delineated (Figs. 6–7).

5. Results

To present the researched results, we visualized the data in QGIS 3.16.16-Hannover. For interpretation of burn severity, we applied the United States Geological Survey (USGS) classification scale (Table 1) with subsequent division into classes. The lower threshold for vegetation affected by fire was set at dNBR = 100. Based on this threshold, the wildfire boundaries were delineated.

As a result, we obtained the following outputs shown in Figures 6 and 7.

Using the “Raster layer unique values report” plugin in QGIS 3.16.16-Hannover, we calculated the burned area sizes according to the USGS classification scale (Table 2 and 3).

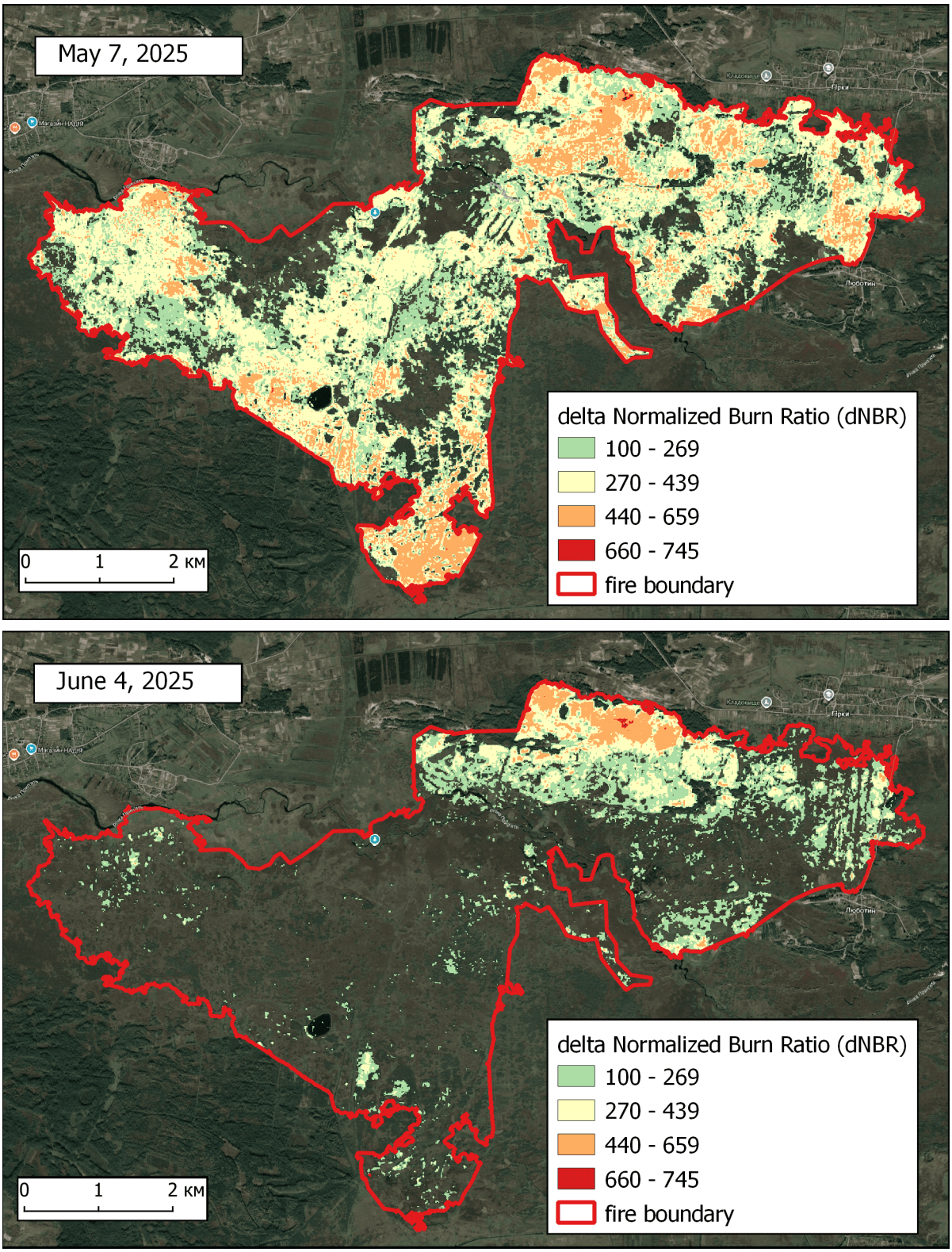

Figure 6: Wildfire aftermath near Birky village (Volyn Region, Ukraine), April 30-May 2, 2025 (dNBR calculated by the authors using Sentinel-2 L2A imagery).

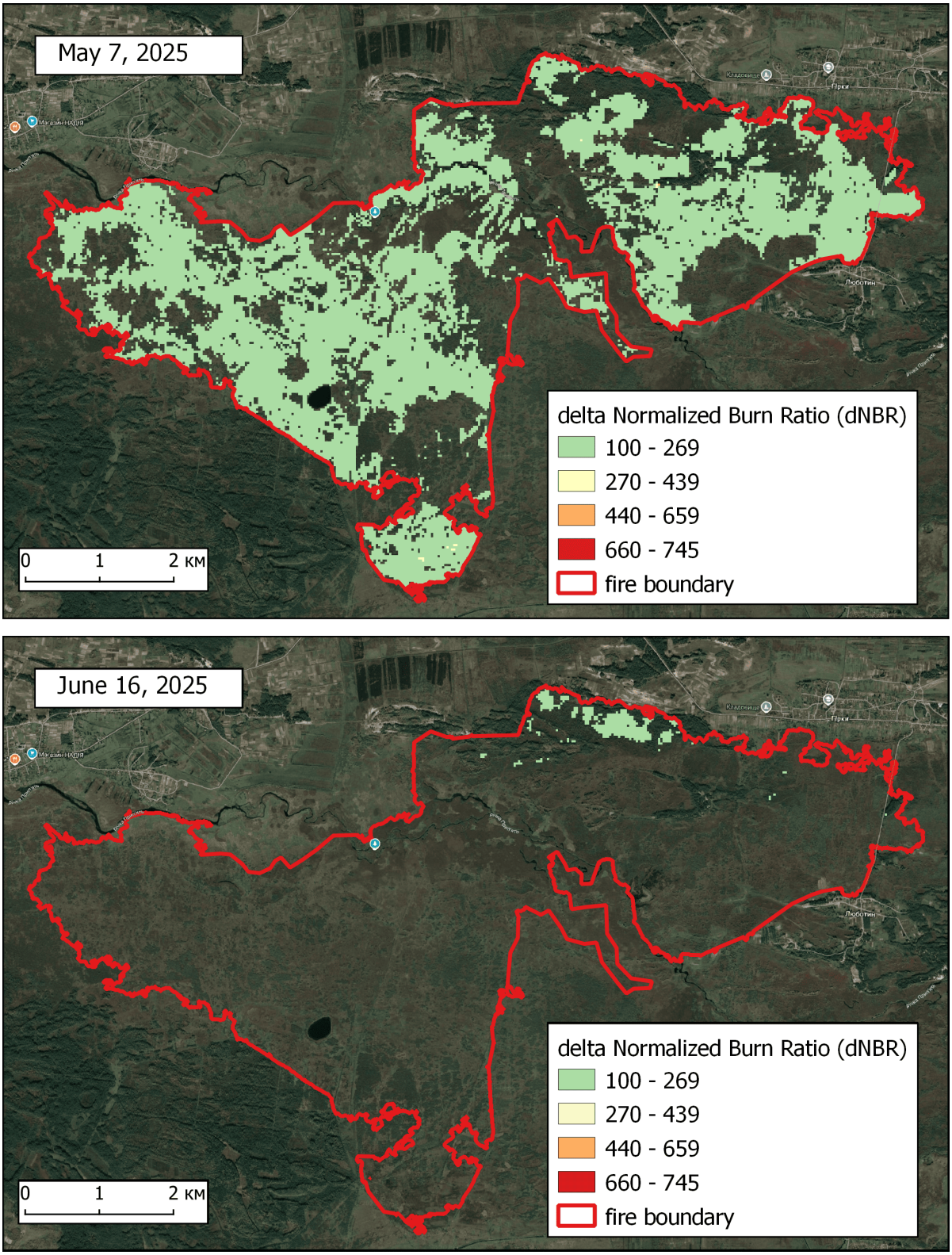

Figure 7: Wildfire aftermath near Birky village (Volyn Region, Ukraine), April 30-May 2, 2025 (dNBR calculated by the authors using Landsat 8-9 OLI/TIRS C2 L1 imagery).

Table 2
Area of burned territories near village Birky, Volyn region, Ukraine (Sentinel-2 L2A)*

Severity level / dNBR	07.05.2025 km^2	%	04.06.2025 km^2	%

Unburned (<100)	9,39	27,5	27,8	80,6
Low severity (100–269)	8,71	25,5	3,99	11,7
Moderate-low severity (270–439)	12,11	35,5	1,88	5,5
Moderate-high severity (440–659)	3,87	11,3	0,74	2,2
High severity (660–745)	0,03	0,1	0,02	0,1
TOTAL	34,11	100	34,11	100

where * – calculated by authors.

Table 3
Area of burned territories near village Birky, Volyn region, Ukraine (Landsat 8-9 OLI/TIRS C2 L1)*

Severity level / dNBR	07.05.2025 km^2	%	16.06.2025 km^2	%
Unburned (<100)	17,29	50,7	33,74	98,9
Low severity (100–269)	16,81	49,3	0,37	1,1
Moderate-low severity (270–439)	0,01	0	–	–
Moderate-high severity (440–659)	–	–	–	–
High severity (660–745)	–	–	–	–
TOTAL	34,11	100	34,11	100

where * – calculated by authors.

6. Discussion

The data obtained show that the wildfire near Birky village, Kamin-Kashyrskyi District, Volyn Region, Ukraine, which lasted from April 30 to May 3, 2025, covered an area of 34.11 km². Despite its massive area, the wildfire's impact was not severe due to the dominance of meadow floodplain vegetation, which is resilient and regenerates quickly.

A major limitation of studies of this kind is access to suitable and relevant satellite imagery. Because the region is frequently cloudy, cloud-free images are often unavailable. As a result, data from multiple satellites must be combined, which complicates interpretation.

Visual analysis of the results shows the presence of "unburned" patches within the wildfire zone on May 7, 2025 (Figs. 6–7). These areas correspond to cloud shadows (Figs. 3–4). Additionally, lakes, open water, and unburned fragments within the burned area distort the overall dNBR distribution. In such cases, dNBR values are inaccurate but do not affect general conclusions. This observation aligns with Bandurka and Svynchuk (2022), who emphasized excluding cloud-covered and water-covered fragments during image interpretation [9].

The highest wildfire intensity occurred in the northern sector near Hirky village, the southern part near Birky, and the western part near Vetly. The northern area, covered with forest, showed the strongest and longest-lasting burn effects. On Sentinel-2 imagery from June 4, 2025, and Landsat 8 imagery from June 16, 2025, fire traces (dNBR > 100) remained visible only in this northern zone (Figs. 6–7).

The wildfire was naturally limited by water bodies – the Prypiat River and nearby drainage channels. Since the study area consists mostly of floodplain meadows and pastures, vegetation damage was minor. Firefighters contained the spread near the villages of Hirky, Birky, Vetly, and Liubotyn.

The dNBR values vary depending on vegetation type, landscape, and local conditions. For more accurate interpretation, field validation is recommended where possible. The dNBR classification ranges are not rigid; threshold shifts of about ±100 points are acceptable. Outliers below -550 or above +1350 may occur in unburned areas due to recognition errors, clouds, or other factors. Settlements also distort results and should be excluded from analysis [13]. To minimize this, we calculated dNBR only within the delineated wildfire contour, using the "Clip raster by mask layer" plugin in QGIS.

Comparison of results from different satellites shows that Sentinel-2 L2A provides more accurate data than Landsat 8–9 OLI/TIRS C2 L1. This is due to its higher spatial resolution (20 m vs. 30 m per pixel) and newer, more sensitive sensor technology. However, since the wildfire had limited ecological impact and its effects largely disappeared within a month, Landsat 8-9 data are sufficiently reliable for most analytical tasks.

Regarding result precision, satellite-based remote sensing cannot be considered high-accuracy. According to Babushka et al. (2021), the deviation in dNBR-based burned area estimation ranges from 6.7% to 11.5% depending on methodology [7].

Our results indicate that within the affected area, low-severity burns dominate: 49.3% according to Landsat 8-9 data; 61.0% (low and moderate-low severity combined) according to Sentinel-2 data. These findings are consistent with Babushka et al. (2021). Overall, the obtained results are sufficiently accurate and suitable for this type of environmental analysis.

7. Conclusions

Thus, remote sensing data processed and analyzed using geographic information systems and technologies are of high importance and great potential for monitoring and preventing adverse natural events such as wildfires. Several online platforms provide near-real-time wildfire data (e.g., FIRMS), which help detect fire occurrences. However, much broader analytical opportunities arise when working directly with satellite imagery.

The most promising approach involves analyzing bands from the near-infrared (NIR) and shortwave infrared (SWIR) ranges, which enable both the detection of active wildfire and the assessment of their long-term environmental effects. Among the numerous available platforms, the Copernicus Browser (European Space Agency) and Earth Explorer (USGS, NASA) offer the most valuable open-access datasets. These were the sources from which we obtained Sentinel-2 L2A and Landsat 8–9 OLI/TIRS C2 L1 imagery for our analysis.

The use of GIS software provides powerful tools for both analysis and visualization. In this study, we used QGIS 3.16.16-Hannover**. The calculation of the **dNBR (Differenced Normalized Burn Ratio)** enabled the evaluation of the long-term environmental impact of the wildfire.

Satellite-derived burn severity maps have strong practical applications. They can support the development of emergency rehabilitation plans and guide vegetation recovery efforts. Furthermore, such data can be used not only to assess burn intensity but also to predict potential secondary effects on burned areas, such as flooding, landslides, or soil erosion.

One of the main challenges in studies of this type is obtaining suitable and cloud-free imagery. Cloud shadows remain a significant obstacle for analysis, especially in regions with frequent cloud cover. In our case, only one fully usable and one conditionally usable image were available within a month after the wildfire, both for Sentinel-2 and Landsat 8–9. This highlights the need for improved methods to work with partially usable imagery and to integrate data from multiple satellite systems within a single analysis.

Further research on wildfires across Ukraine using remote sensing data is urgently needed. Such studies should aim to identify regional patterns, refine (calibrate) the USGS burn severity scale for different landscapes and vegetation types, and evaluate the accuracy of burn severity analysis across various satellite platforms.

Declaration on Generative AI

The authors have not employed any Generative AI tools.

References

[1] F. Sivrikaya, B. Saglam, A. E. Akay, N. Bozali, Evaluation of forest fire risk with GIS, Pol. J. Environ. Stud. 23 (2014) 187–194. URL: https://www.researchgate.net/publication/288597149_Evaluation_of_Forest_Fire_Risk_with_GIS.

[2] R. K. Jaiswal, S. Mukherjee, K. D. Raju, R. Saxena, Forest fire risk zone mapping from satellite imagery and GIS, Int. J. Appl. Earth Obs. Geoinf. 4 (2002) 1–10. doi:10.1016/S0303-2434(02)00006-5.

[3] E. Chuvieco, J. Salas, Mapping the spatial distribution of forest fire danger using GIS, Int. J. Geogr. Inf. Syst. 10 (1996) 333–345. doi:10.1080/02693799608902082.

[4] A. Supriadi, T. Oswari, Analysis of geographical information system (GIS) design application in the fire department of Depok City, Technium Soc. Sci. J. 8 (2020) 1–7. doi:10.47577/tssj.v8i1.181.

[5] H. Adab, K. D. Kanniah, K. Solaimani, Modeling forest fire risk in the northeast of Iran using remote sensing and GIS techniques, Nat. Hazards 65 (2013) 1723–1743. doi:10.1007/s11069-012-0450-8.

[6] V. Zatserkovnyi, P. Savkov, I. Pampukha, K. Vasetska, Application of GIS and remote sensing of the Earth for the forest fire monitoring, Visnyk Taras Shevchenko Natl. Univ. Kyiv. Mil.-Spec. Sci. 2 (2020) 54–58. doi:10.17721/1728-2217.2020.44.54-58.

[7] A. Babushka, L. Babiy, B. Chetverikov, A. Sevruk, Research of forest fires using remote sensing data (on the example of the Chornobyl exclusion zone), Geod. Cartogr. Aerophotogr. 94 (2021) 35–43. doi:10.23939/istcgcap2021.94.035.

[8] O. I. Borysenko, V. L. Meshkova, Forecasting the spread of fires and harmful insect populations in pine forests using GIS, Planeta-Print, Kyiv, Ukraine, 2021.

[9] O. Bandurka, O. Svynchuk, Method of identification of space images for forecasting forest fires, Control Navig. Commun. Syst. 1 (2022) 13–18. doi:10.26906/sunz.2022.1.013.

[10] Copernicus Browser, 2025. URL: https://browser.dataspace.copernicus.eu/.

[11] EarthExplorer, 2025. URL: https://earthexplorer.usgs.gov/.

[12] European Space Agency, Copernicus browser guide, 2025. URL: https://www.esa.int/Education/Copernicus_Browser_guide.

[13] Office for outer space affairs, normalized burn ratio (NBR), UN-SPIDER recommended practices, 2025. URL: https://un-spider.org/advisory-support/recommended-practices/recommended-practice-burn-severity/in-detail/normalized-burn-ratio.

[14] C. H. Key, N. C. Benson, Landscape assessment (LA): sampling and analysis methods, Technical Report, U.S. Department of Agriculture, Forest Service, 2025. URL: https://www.fs.usda.gov/rm/pubs_series/rmrs/gtr/rmrs_gtr164/rmrs_gtr164_13_land_assess.pdf.

[15] S. Pugach, O. Kaidyk, T. Terletskyi, D. Uhryn, O. Visyn, GIS tools for analysis and modeling of emergency situations (on the example of fires in Volyn region), Comput.-Integr. Technol.: Educ. Sci. Prod. (2025) 466–475. doi:10.36910/6775-2524-0560-2025-60-49.

[16] FIRMS, Tutorials & examples, 2025. URL: https://firms.modaps.eosdis.nasa.gov/tutorials/.

[17] FIRMS, Global fire map, 2025. URL: https://firms.modaps.eosdis.nasa.gov/map.

[18] SentinelHub, Fire boundary script, 2025. URL: https://custom-scripts.sentinel-hub.com/sentinel-2/fire_boundary/.